

Vortex Shedding on Combined Bodies at Incidence to a Uniform Air Stream

T. Yavuz^x, Y. E. Akansu^{xx}, M. Sarioğlu^{xxx}, and M. Özmert^{xx}

^x. Başkent University, ^{xx}: Nigde University, ^{xxx}: Karadeniz Technical University, Turkey

Abstract—Vortex-shedding phenomenon of the flow around combined two bodies having various geometries and sizes has been investigated experimentally in the Reynolds number range between 4.1×10^3 and 1.75×10^4 . To see the effect of the rotation of the bodies on the vortex shedding, the combined bodies were rotated from 0° to 180° . The combined models have a cross section composing of a main circular cylinder and an attached circular or square cylinder. Results have shown that Strouhal numbers for two cases were changed considerably with the angle of incidence, while it was found to be largely independent of Reynolds number at $\theta \leq 150^\circ$. Characteristics of the vortex formation region and location of flow attachments, reattachments, and separations were observed by means of the flow visualizations. Depending on the inclination angle the effects of flow attachment, separation and reattachment on vortex-shedding phenomenon have been discussed.

Keywords—Bluff body, vortex shedding, flow separation, flow reattachment.

I. INTRODUCTION

Flows around circular cylinder and square prism as basic geometries, have been investigated by many workers for a long time. Such bluff bodies often applied in the form of groups in many cases of engineering practices. In these cases, flow characteristics of such objects in contact or in close proximity show major differences, because of the interactions with each other, according to those of single applications. Therefore, numerous investigators have been interested in flow past two bodies which have same or different shapes.

Fleck [1] investigated the flow past a combined body, composed of a circular cylinder and a rectangular prism, in the Reynolds number range from 1×10^4 to 5×10^4 . It was found that the observed Strouhal number is independent of Reynolds number for the range of angle of attack $-90^\circ \leq \alpha \leq 45^\circ$. In effect, the sharp corners of the rectangular portion dominate the vortex shedding mechanism for the majority of the range of the angle of attack. The only range where there is Reynolds number dependence is $45^\circ \leq \alpha \leq 90^\circ$, when the rectangular body is largely in the wake of the circular body. In this case, the presence of the rectangular body on the downstream side

of the circular cylinder considerably affects the location of the separation point.

Wei and Chang [2] studied flow characteristic of wake and base-bleed flow downstream of two bluff bodies, with different geometries, arranged side by side. The two-body arrangements are comprised of flat plate-square cylinder, flat plate-circular cylinder, and square cylinder-circular cylinder. In this study, they used two sets of models, these being bluff bodies with the same cross sectional dimension but with different vortex shedding frequencies, and bluff bodies with different cross sectional dimension but with the same vortex shedding frequencies. It is suggested that when the gap distance is small, the vortex shedding frequency downstream of the two body arrangement is about half of the average of the shedding frequencies that correspond to each single bluff body.

Luo and Gan [3] investigated the structure associated with flow past two tandem circular cylinders with a diameter ratio of 0.33 and with the smaller cylinder upstream. Just like the case of flow past two equal size cylinders, a critical spacing was found to exist. For spacing less than the critical value, share layers that separate from the upstream cylinder reattach onto the downstream cylinder whereas for spacing larger than the critical value both cylinders shed vortices.

In the study of Igarashi [4], experimental investigations on the characteristics of a flow around two circular cylinders of different diameters with the ratio $d_2/d_1=0.68$ arranged in tandem were carried out. The flow patterns vary with an increasing of the spacing of the axes of the cylinders in the same manner as in the case of equal diameters. The pattern in which the spacing of the axes of the cylinders was the smallest (this case is closest to our present case) is a complete separation type in which the separated shear layer from the first cylinder does not reattach onto the second one.

Tsutsui et al. [5] studied experimentally and numerically the behavior of an interactive flow around two circular cylinders with different diameters ($d/D=0.45$) at close proximity. In particular, the reattachment that the separated share layer from the main cylinder reattaches on the rear surface by Coanda effect was mentioned.

In the study of Gu and Sun [6], the interference between two identical circular cylinders arranged in staggered configurations has been investigated at high subcritical Reynolds numbers. In general, three different pressure

^x : Corresponding autor

distribution patterns on the downstream cylinder and two switching processes were observed for the wind angle varying from 0° (in tandem) to 90° (in side by side). The corresponding flow patterns were classified as wake, share layer and neighbourhood interference respectively.

For different forebody sections, vortex sheddings from bluff bodies with emphasis on finding the effects of afterbody shape were experimentally investigated by Nakamura [7]. It was found that the Strouhal number of a bluff body with afterbody decreases initially with increasing side ratio in which one of the most important shape parameters for controlling the Strouhal number is the ratio of afterbody length to cross-flow dimension of the bluff body. This is in sharp contrast to the base suction that is sensitively dependent of afterbody shape. Nakamura [8] also experimentally studied the effect of the extended splitter plates on the bluff bodies with forebody shapes. These forebody shapes examined included a circular shape, a semi-circular section with and without a rectangular block and a normal flat plate. It was shown that vortex shedding from bluff bodies with extended splitter plates is characterized by the impinging-shear-layer instability, where the Strouhal number in terms of splitter plate length increases with increasing splitter plate length.

Akansu et al. [9] investigated experimentally the behavior of a stationary circular cylinder with an attached plate, under conditions where the entire cylinder-plate body was to rotate about the cylinder axis, in the Reynolds number of 2×10^4 . The results indicate that the shedding frequency was nearly constant in the range of the plate angle of $50^\circ - 120^\circ$ and as farther increasing the angle from 120° to 160° , it strikingly increases and then again decreases at the angles bigger than 160° deg. The plate also causes important changes in pressures on the surface of the cylinder depending on the flow separation and reattachment as increasing the inclination angle. A similar study for a square prism with an attached plate was made by Sarioglu et al. [10]. Their results indicated that the Strouhal number based on D , the side length of the square cylinder, has a strong peak at $\theta = 12^\circ$ and drag coefficient of the square cylinder has minimum and maximum values at approximately $\theta = 20^\circ$ and 80° respectively.

Based on the results summarized above, it can be concluded that flow around two adjacent bluff bodies depends strongly on the geometries and the angle of incidence. Therefore, the present study focused on the investigation of the flow around combined bluff bodies with different cross-sectional geometries at incidence. Two combined models used as a main circular cylinder ($D=9.5$ mm) with an attached small cylinder having circular cylinder ($d=6$ mm) or square prism ($d=6$ mm).

II. EXPERIMENTAL APPARATUS AND PROCEDURE

The experiments were conducted in the test section of a blower type open jet TE 44 subsonic wind tunnel having working cross section of 457 mm x 457 mm. Boundary layer correction is achieved by corner fillets extending the length of

the contraction cone and the working section, proportioned to ensure a uniform longitudinal pressure in the working section. At the maximum tunnel speed of about 30 m/s, the free stream turbulence intensity was about 0.5% ; the turbulence intensity was higher at low tunnel speeds, about 1.5% at 4 m/s, which is the lowest speed in the tunnel. The Reynolds number based on the diameter of the main cylinder, D , was ranged between 4.1×10^3 and 1.75×10^4 . The tunnel and test section are shown in Fig. 1.

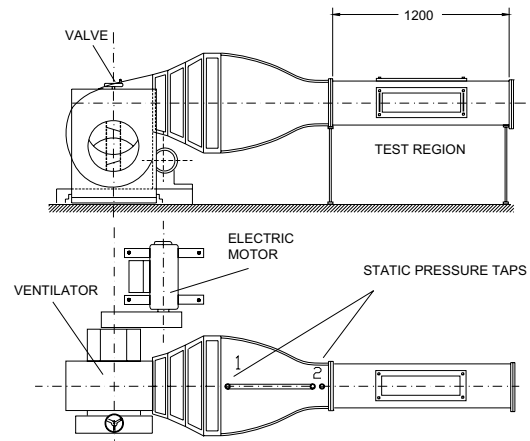


Fig. 1 Blower type open jet subsonic wind tunnel and test section.

The test models consisted of two configurations are shown in Fig. 2. As shown in the figure, the upstream cylinders having circular and square cross sections were combined with the main circular cylinder in a line contact at the center axis. The side length of the square cylinder ($d=6$ mm) and the diameter of the main circular cylinder ($D=9.5$ mm) were chosen to ensure the vortex shedding frequencies of both square and circular cylinders to be same when they stay isolated in the flow. All models were made from stainless steel and the square prism was machined sharp edges. The lengths of the bodies are same with the width of the tunnel test section and they spanned the entire width of the test section.

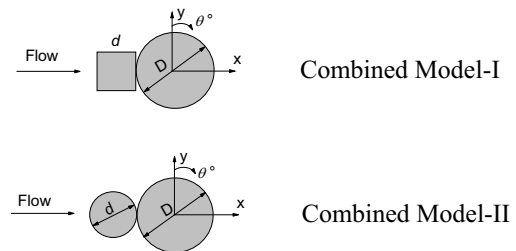


Fig. 2 Two different combined model geometries and coordinate system.

The combined models were centered on the mid-height of the test section and they were positioned at an angle of incidence to the free-stream flow direction and turned in the range of $0^\circ \leq \theta \leq 180^\circ$ with an increment of 3° , with an accuracy of $\pm 0.5^\circ$. Maximum solid blockage ratios of the combined models are, 3.48% for the Model-I at $\theta = 75^\circ$ and

105°, and 3.39 % for the Model-II at $\theta = 90^\circ$. As the blockage ratios are smaller than 6.0 %, no correction was made for the blockage effects [11]. Minimum aspect ratios based on the projected cross stream dimension of the models are 29.5 for the Model-I and II. It can be said that these aspect ratios are satisfactory for a bluff body to be treated as two dimensional [2].

Vortex sheddings from the test models were detected by using a TSI IFA 100 model constant temperature anemometer with two hot-film probes. The Strouhal numbers for the vortex shedding from the models were determined from the frequency analysis of the velocity fluctuations. The probes were located at the position of $x/D = 5$ and 15 , $y/D = \pm 2.5$, where x/D and y/D are the downstream and vertical distances respectively, in the downstream of the body. The hot-film probes were calibrated using a TSI Model 1125 calibrator. The frequency response for the hot-film probes were found to be about 20 kHz by using a square wave test. The velocity measurements were carried out using a computer controlled data acquisition system. For velocity measurements at each measurement point, 4096 data were acquired at a sampling rate of 4 kHz using a low-pass filter setting of 2000 Hz. So the measuring time corresponded to 1.024 s. TSI Thermal-Pro Software was used to acquire signals with a 12 bit A/D converter and to obtain the statistical and spectral analyze of these measurement signals.

Flow visualization experiments were conducted by using a smoke-wire method in the different wind tunnel for Reynolds number of 5.0×10^3 . In these experiments, three times bigger test model dimensions have been used to obtain a Reynolds number to be in the range of Reynolds number used in the velocity measurements.

The experimental uncertainty in the measurement of velocity was determined to be less than $\pm 3\%$, whereas those of the Strouhal number and the frequency spectra calculated from the experimental measurements were determined to be less than $\pm 3.3\%$ and $\pm 0.5\%$, respectively.

III. EXPERIMENTAL RESULTS AND DISCUSSION

The vortex sheddings from the models were examined in the Reynolds number between 4.1×10^3 and 1.75×10^4 . A sample velocity spectra distribution obtained for the Model-I, at the Reynolds number 9×10^3 is given in Fig. 3. It is quite clear that, with increasing θ from 0° , there is a sharply decrease in vortex shedding frequency up to $\theta = 24^\circ$, then this decrease in shedding frequency slightly continues up to 48° . After 84° , it gradually increases up to 168° and then it decreases again.

Using vortex-shedding frequencies obtained from spectral distributions, the Strouhal numbers, St based on D and St' based on D' , calculated for the Models I and II at the three Reynolds number 4.1×10^3 , 9.0×10^3 and 1.5×10^4 are shown in Figs. 4 and 5. As shown in Fig. 4, at $\theta = 0^\circ$ the value of St' is about 0.25 and this value is above of that of the single circular cylinder. This indicates that the shear layers separated from

the leading edges of the square cylinder goes very near main cylinder of the Model-I and causes to narrow wake than that of the single circular cylinder. The Strouhal number decreases sharply from 0° to 15° . Because, the shear layers separated from the corner A and B roll rear of the model without a reattachments on the cylinder and with a more wide wake. The Strouhal number increases gradually with the rotation of the Model-I in the range between 15° – 69° . This increase in St' quietly depends on the reattachment of the separated shear layer from corner B on the face AB. As the angle approaches 69° , this reattachment point closes to the corner A and, so it is seen a peak in the Strouhal number. After this angle, the separated shear layer from the corner B does not reattach on the face AB anymore and causes a sudden increase in the width of the wake and consequently the Strouhal number decreases. This phenomenon implies the existence of a decrease in the Strouhal number. This decrease proceeds until about 90° in which the width of the wake reaches its maximum value. As the angle farther increases, the Strouhal number increases gradually up to 168° in which the Strouhal number shows a peak for the Reynolds numbers 4.1×10^3 and 9×10^3 . Approaching this angle, a reattachment occurs again on the square cylinder. After 168° , there is a sudden decrease in Strouhal number due to giving up this reattachment and also reducing the width of the wake. For $Re = 1.5 \times 10^4$, the peak in the Strouhal number occurs at 174° . This is associated with the variation of the separation point on the circular cylinder with the Reynolds number. As a matter of fact, in the study of Fleck [1], Strouhal number changes with the Reynolds number strikingly especially in the case where the circular cylinder is upstream.

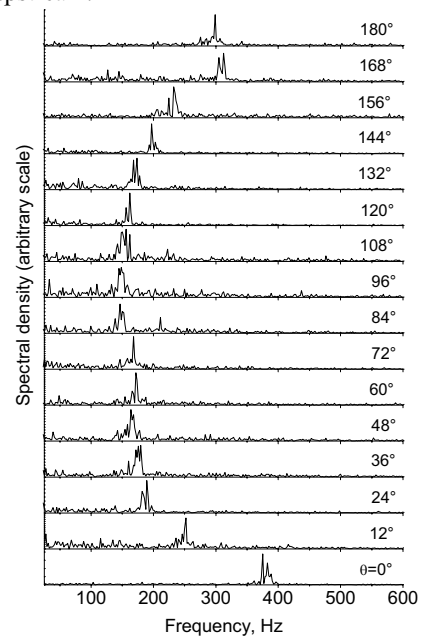


Fig. 3 Spectra measured at $x/D = 15$, $y/D = 2.5$ in the wake of the Model-I ($Re = 9.0 \times 10^3$).

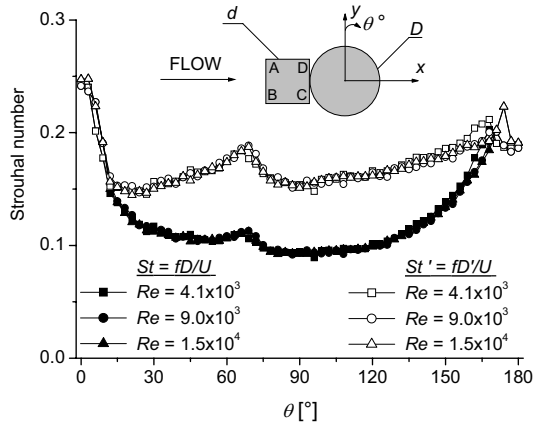


Fig. 4 Strouhal number vs rotation angle, θ for the Model-I.

Strouhal numbers for the Model-II are presented in Fig. 5. In this case, as the smaller body has circular shape, the Reynolds number effects are noticed in the range of θ , 0° – 12° , unlike the other model. At $\theta = 0^\circ$, the value of the Strouhal Number for the $Re=4.1 \times 10^3$ is above of those for the $Re=9.0 \times 10^3$ and 1.5×10^4 . For the case of $Re=4.1 \times 10^3$, at the beginning ($\theta = 0^\circ$), the shear layer separated from the small cylinder reattaches on the downstream cylinder and this reattachment continues, with the small change in the location of the separation point on the big cylinder, until $\theta = 12^\circ$. After 12° , a sudden decrease in the Strouhal number occurs by ending the reattachment. For the case of $Re=1.5 \times 10^4$, there is no reattachment at the beginning. With increasing the angle of incidence up to 12° , the Strouhal number increases because of the reattachment occurring on the lower side of the Model-II. Here, also after $\theta = 12^\circ$, the reattachments give up and the Strouhal number decreases suddenly. In the range of $\theta = 15^\circ$ – 150° , unlike the Model-I having sharp edges, there is no peak in Strouhal number. After 150° , the variation of the Strouhal number is similar to those of the Model-I because of changing the position of the main cylinder from downstream to upstream, and consequently the flow under consideration is in the influence of the main circular cylinder.

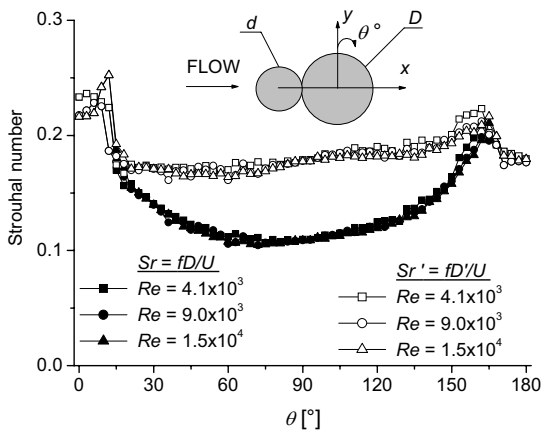


Fig. 5 Strouhal number vs incidence angle θ for the Model-II

To examine the flow field about the Model-II arrangement, flow visualization experiments were conducted by using a smoke-wire method in the wind tunnel for $Re=5 \times 10^3$. In Fig. 6, the positions of flow attachment, separation, and reattachment on the two combined circular cylinders due to the inclination of the body can be clearly seen. The variation of vortex formation region behind the bodies can be also seen in this figure. When the flow pattern of the Model-II at $\theta = 0^\circ$ is compared with the case of $\theta = 180^\circ$, there are considerable changes in the wake, and the distance required for vortex formation behind the bodies varies. Narrow wake causes more small vortices and higher vortex shedding frequencies.

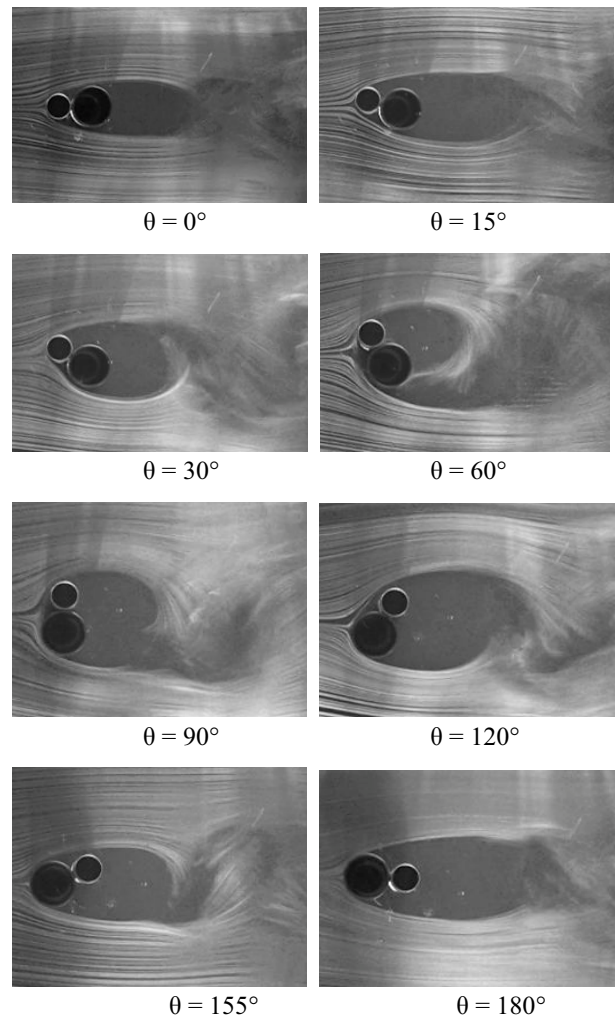


Fig. 6 Smoke-wire visualization of the flow around test Model-II for $Re = 5 \times 10^3$

Fig. 7 shows Strouhal number as a function of Reynolds number for various angles of incidence considered for the Model-I. It can be said that the Strouhal number was found to be largely independent of Reynolds number up to $\theta \leq 100^\circ$. In the range of 160° – 175° , Strouhal number has an unstable variation with Reynolds number in $Re < 7.5 \times 10^3$. This situation was also seen in Fig 4.

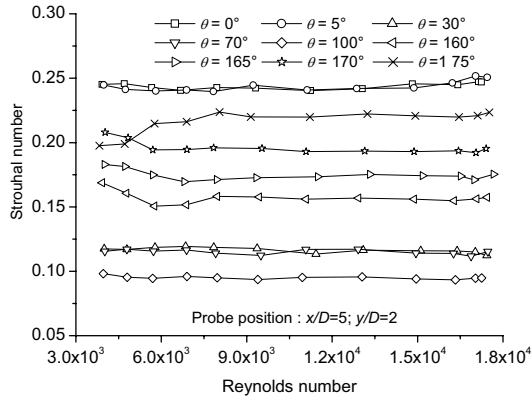


Fig. 7 Distribution of Strouhal number of the Model-I vs Reynolds number for different angles of incidence.

A summarized classification of the flow regimes of the two combined test models is shown in Fig. 8. The flow structures mentioned above are presented schematically in this figure. Here, flow attachments, separations and reattachments and their behaviors according to the angle of incidence are shown.

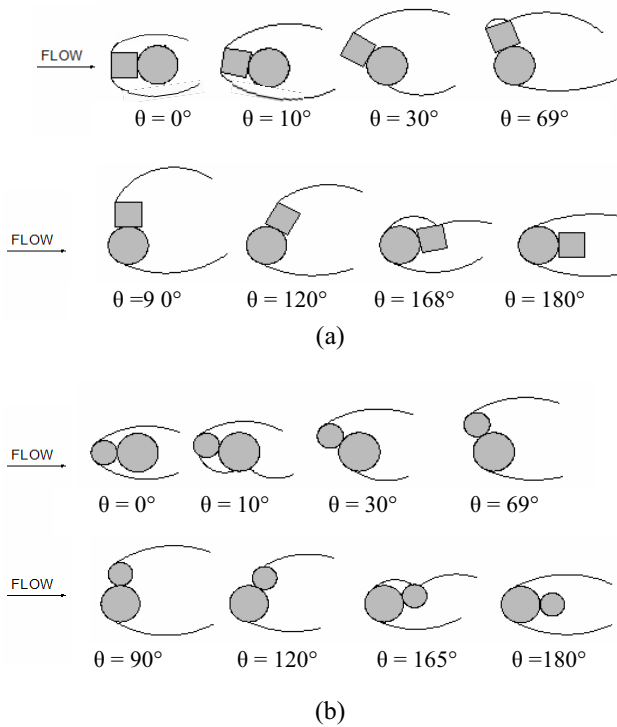


Fig. 7 Assumed flow patterns around the combined models for $Re=9.0 \times 10^4$ a) Model-I, b) Model-II

IV. CONCLUSION

Vortex-shedding phenomenon in the flow around two different combined models at incidence has been investigated experimentally in the Reynolds number range of 4.1×10^3 and 1.75×10^4 . The following conclusions were obtained:

The Strouhal numbers for two combined models considered were changed strikingly with the angle of incidence, whereas

it was found to be largely independent of Reynolds number at $\theta \leq 150$ deg. For both of the models, the Strouhal number increase at the angles of incidence in which reattachments occur. By the end of reattachments, the width of the wake increases and Strouhal number decreases suddenly. The peak appeared in Strouhal number at about $\theta = 60^\circ$ in the case of sharp edged square model have not seen in the case of Model-II which is composed of two circular cylinders.

NOMENCLATURE

Symbol	Quantity
D	diameter of the bigger circular cylinder
D'	the projected cross stream dimension of the combined bodies
d	small dimension of the upstream bodies
f	vortex-shedding frequency
R	Reynolds number based on $D, UD/\nu$
St	Strouhal number, fD/U
St'	Strouhal number, fD'/U
U	freestream velocity
w	the length of the big side of the rectangular body
x, y	streamwise and lateral coordinates
θ	inclination angle of the combined models
ν	kinematic viscosity of fluid
ρ	density of air

REFERENCES

- [1] B. A. Fleck, "Strouhal Numbers for Flow past a Combined Circular-Rectangular Prism," *Journal of Wind Engineering and Industrial Aerodynamics*, vol. 89, 2001, pp. 751-755.
- [2] Y. C. Wei and J. R. Chang, "Wake and Base-Bleed Flow Downstream of Bluff Bodies with Different Geometry," *Experimental Thermal and Fluid Science*, vol. 26, 2002, pp. 39-52.
- [3] S. C. Luo and T. L. Gan, "Flow past 2 Tandem Circular-Cylinders of Unequal Diameter," *Aeronautical Journal*, vol. 6, No. 953, 1992, pp. 105-114.
- [4] T. Igarashi, "Characteristics of a Flow around Two Circular Cylinders of Different Diameters Arranged in Tandem," *Bulletin of the JSME*, vol. 25, No. 201, 1982, pp. 349-357.
- [5] T. Tsutsui, T. Igarashi, and K. Kamemoto, "Interactive Flow around two Circular Cylinders of Different Diameters at Close Proximity. Experiment and Numerical Analysis by Vortex Method," *Journal of Wind Engineering and Industrial Aerodynamics*, vol. 69, no. 71, 1997, pp. 279-291.
- [6] Z. Gu and T. Sun, "On Interference between two Circular Cylinders in Staggered Arrangement at High Subcritical Reynolds Numbers," *Journal of Wind Engineering and Industrial Aerodynamics*, vol. 80, 1999, pp. 287-300.
- [7] Y. Nakamura, "Vortex Shedding From Bluff Bodies and a Universal Strouhal Number," *Journal of Fluids and Structures*, vol. 10, 1996, pp. 159-171.
- [8] Y. Nakamura, "Vortex Shedding From Bluff Bodies with Splitter Plates," *Journal of Fluids and Structures*, vol. 10, 1996, pp. 147-158.
- [9] Y. E. Akansu, M. Sarioglu, and T. Yavuz, "Flow Around a Rotatable Circular Cylinder-Plate Body at Subcritical Reynolds Numbers," *AIAA Journal*, vol. 42, no. 6, June 2004, pp. 1073-1080.
- [10] M. Sarioglu, Y. E. Akansu, and T. Yavuz, "Flow Around a Rotatable Square Cylinder-Plate Body," *AIAA Journal*, vol. 44, no. 5, May 2006, pp. 1065-1072.
- [11] G. S. West and C. J. Apelt, "The Effects of Tunnel Blockage and Aspect Ratio on the Mean Flow Past a Circular Cylinder with Reynolds Numbers between 10^4 and 10^5 ," *J. Fluid Mech.*, vol. 114, 1982, pp. 361-377.